# Grain orientation dependence of deformation microstructure evolution and mechanical properties in face-centered cubic high/medium entropy alloys

To cite this article: S Yoshida *et al* 2022 *IOP Conf. Ser.: Mater. Sci. Eng.* **1249** 012027



# Grain orientation dependence of deformation microstructure evolution and mechanical properties in face-centered cubic high/medium entropy alloys

**S Yoshida[1,2*], R Fu[3], W Gong[4], T Ikeuchi[1], Y Bai[2,5], Z Feng[3], G Wu[3], A Shibata[2,6], N Hansen [7], X Huang[3], and N Tsuji[1,2]**

[1] Department of Materials Science and Engineering, Kyoto University, Kyoto, Japan
[2] Elements Strategy Initiative for Structural Materials (ESISM), Kyoto University, Kyoto, Japan
[3] International Joint Laboratory for Light Alloys (MOE), College of Materials Science and Engineering, Chongqing University, Chongqing, China.
[4] J-PARC Center, Japan Atomic Energy Agency, Tokai, Ibaraki, Japan
[5] School of Materials Science and Engineering, Dalian University of Technology, Dalian, China
[6] Research Center for Structural Materials, National Institute for Materials Science, Tsukuba, Ibaraki, Japan
[7] Technical University of Denmark, Risø campus, Roskilde, Denmark

E-mail: yoshida.shuhei.5s@kyoto-u.ac.jp

**Abstract**. This study revealed characteristics of the deformation behavior in high/medium entropy alloys (HEAs/MEAs) with face-centered cubic (FCC) structure. A $Co_{60}Ni_{40}$ alloy and a $Co_{20}Cr_{40}Ni_{40}$ MEA having low and high friction stresses (fundamental resistance to dislocation glide in solid solutions), respectively, but similar in other properties, including their stacking fault energy and grain sizes, were compared. The MEA exhibited a higher yield strength and work-hardening ability than those in the $Co_{60}Ni_{40}$ alloy at room temperature. Deformation microstructures of the $Co_{60}Ni_{40}$ alloy were composed of coarse dislocation cells (DCs) in most grains, and a few deformation twins (DTs) formed in grains with tensile axis (TA) nearly parallel to <111>. In the MEA, three microstructure types were found depending on the grain orientations: (1) fine DCs developed in TA~//<100>-oriented grains; (2) planar dislocation structures (PDSs) formed in grains with other orientations; and (3) dense DTs adding to the PDSs developed in TA~//<111>-oriented grains. The results imply difficulty in cross-slip of screw dislocations and dynamic recovery in the MEA, leading to an increase in the dislocation density and work-hardening rate. Our results suggest that FCC high-alloy systems with high friction stress inherently develop characteristic deformation microstructures advantageous for achieving high strength and large ductility.

## 1. Introduction

High entropy alloys (HEAs) and medium entropy alloys (MEAs) are novel classes of solid solution alloys having five or more and four or fewer constituent elements, respectively, with near equiatomic fractions [1,2]. Among such systems, HEAs and MEAs with face-centered cubic (FCC) structures have been known to exhibit an exceptional balance of strength and ductility in a wide range of temperatures (from room temperature to cryogenic temperatures) [3,4]. Our previous studies revealed that FCC HEAs

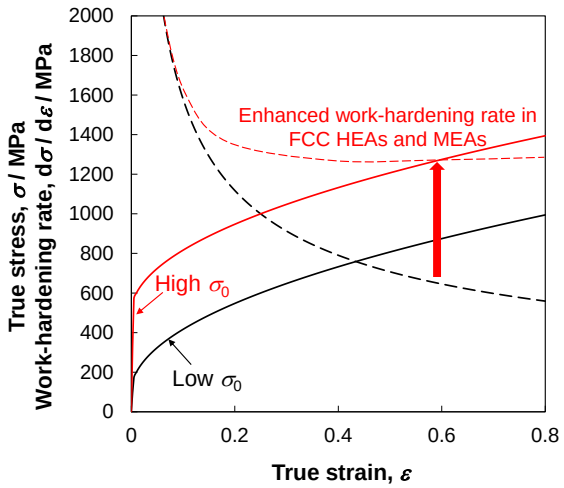


**Figure 1.** True stress-true strain curves of virtual alloys with high (red solid curve) and low (black solid curve) friction stresses, $\sigma_0$. Their work-hardening rate curve as a function of true strain is also shown by a black dashed curve. The red dashed curve indicates the typical work-hardening rate of FCC HEAs and MEAs observed experimentally.

and MEAs showed significantly high friction stress, $\sigma_0$, (fundamental resistance to dislocation motion in solid solutions), contributing to their high yield strength and high tensile strength [5–7]. It remains a question as to whether the excellent strength-ductility balance of FCC HEAs and MEAs can be explained simply based on the enhanced strength by their high $\sigma_0$. To examine this question, we now conduct a simple thought experiment. Figure 1 shows tensile true stress-true strain curves of virtual FCC alloys with low $\sigma_0$ (black solid curve) and high $\sigma_0$ (red solid curve). It is assumed that the same deformation mechanisms (e.g., activated slip systems and/or deformation twinning systems) operate in these two alloys, and they have identical elastic properties. Accordingly, the work-hardening rate curves of these two alloys are identical (dashed black curve). In general, uniform elongation of strain-rate insensitive materials can be determined by the plastic instability condition [83], expressed by the Considère equation [8]:

$$\frac{d\sigma}{d\varepsilon} \leq \sigma. \quad (1)$$

When the work-hardening rate becomes equal to the flow stress (corresponding to the crossover of the true stress-true strain curves and the work-hardening curve), macroscopic necking is initiated according to equation (1), leading to fracture. From figure 1, we can understand that the uniform elongation of the alloy with high $\sigma_0$ is smaller than that of the alloy with low $\sigma_0$ under the identical work-hardening rate. Therefore, it can be concluded in this thought experiment that an increase in the friction stress leads to degradation of the strength-ductility balance, unless the work-hardening rate increases. This means that the strength-ductility balance of FCC HEAs and MEAs (with high $\sigma_0$) is worse than that in other conventional dilute FCC alloys (with low $\sigma_0$), contradictory to the excellent mechanical properties observed in reality [3,4]. Thus, we hypothesize that, in FCC HEAs and MEAs, there exists a mechanism to enhance their strength and ductility simultaneously (i.e., enhanced work-hardening ability as indicated by the red dashed curve in figure 1). To validate this idea, we have investigated the deformation behavior of a $Co_{20}Cr_{40}Ni_{40}$ MEA with high $\sigma_0$ (280 MPa) and a $Co_{60}Ni_{40}$ binary model alloy with low $\sigma_0$ (52 MPa) where these alloys are similar in other materials properties, such as elastic constants, lattice constants, melting points, and stacking fault energies (SFEs) [9,10].

## 2. Experimental methods

Ingots of the $Co_{60}Ni_{40}$ alloy and $Co_{20}Cr_{40}Ni_{40}$ MEA were cast by a vacuum arc-melting of high purity elements (99.9 wt.%). The ingots were then homogenized at 1100 ºC for 24 h and rapidly cooled by water quenching. The homogenized $Co_{60}Ni_{40}$ alloy and $Co_{20}Cr_{40}Ni_{40}$ MEA were cold-rolled by a

reduction of 92% in thickness and subsequently heat-treated at 750 ºC for 120 s and 850 ºC for 3.6 ks, respectively. This produced fully-recrystallized microstructures with mean grain sizes of approximately 3 μm, including annealing twin boundaries. To evaluate their mechanical properties, tensile specimens with a gauge dimension of 2 mm (length) × 1 mm (width) × 0.5 mm (thickness) were cut from the recrystallized materials, and tensile tests were carried out at a quasi-static strain rate of $8.3 \times 10^{-4}$ $s^{-1}$ at room temperature. The surface of the specimens was painted with white and black ink to produce random dot patterns. The displacement of the gauge section was precisely measured by tracking the patterns using a CCD video camera extensometer, and the strain was calculated using the digital image correlation (DIC) technique [11]. We have previously confirmed that tensile tests using such small specimens with DIC measurements give stress-strain data equivalent to those obtained using standard-sized specimens [5,6]. The tensile deformation was interrupted at different strain levels, and the deformation microstructures of the materials were characterized by transmission electron microscopy (TEM) equipped with bright-field (BF) and annular dark-field (ADF) detectors for scanning transmission electron microscopy (STEM). The TEM/STEM observations were conducted at an acceleration voltage of 200 kV under two-beam conditions as described in Ref. [12]. The crystallographic orientations (crystal direction) parallel to the tensile axis in each grain were determined based on Kikuchi patterns obtained by convergent beam electron diffraction. In each material, more than 20 grains from two thin foils were observed, confirming the reproducibility of the results.

## 3. Results and discussion

Figure 2 shows true stress-true strain curves obtained for the $Co_{60}Ni_{40}$ alloy and $Co_{20}Cr_{40}Ni_{40}$ MEA. The MEA exhibited higher yield strength (375 MPa) than the $Co_{60}Ni_{40}$ alloy (140 MPa) owing to the higher friction stress of the MEA. Based on the slopes of the true stress-true strain curves, the work-hardening rate of the MEA was found to be higher than the $Co_{60}Ni_{40}$ alloy, leading to their fracture at almost the same strain levels. Therefore, it was concluded that the MEA exhibited a better strength-ductility balance.

To reveal the reasons for the difference in deformation behaviors in those two alloys, we investigated the evolution of their deformation microstructures. As demonstrated in previous studies [13,14], the evolution of deformation microstructures in FCC metals is grain-orientation dependent. Therefore, we classified the types of deformation microstructures depending on the grain orientation against the tensile axis (TA). Figure 3 (a) shows an example of the deformation microstructures showing dislocation cells (DCs) in the $Co_{60}Ni_{40}$ alloy. Coarse DCs with a size of several hundred nanometers developed in most grains of the $Co_{60}Ni_{40}$ alloy regardless of grain orientation. In a small number of grains oriented to TA ~// <1 1 1>, a few deformation twins were found, as shown in figure 3 (b), in addition to DCs slightly finer than those in figure 3 (a). In the $Co_{20}Cr_{40}Ni_{40}$ MEA, three distinct types of deformation

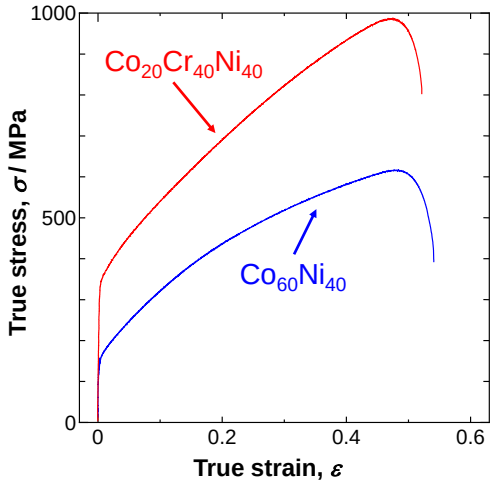


**Figure 2.** True stress-true strain curves for the $Co_{60}Ni_{40}$ alloy and $Co_{20}Cr_{40}Ni_{40}$ MEA obtained by tensile tests at room temperature.

microstructures were found to be developed. Figure 4 (a) shows an example of fine DCs with a size of several tens of nanometers in grains oriented to TA ~// <1 0 0>. In the case of grains with other orientations, characteristic planar dislocation structures (PDSs) parallel to specific {1 1 1} planes were formed, as shown in figure 4 (b). This suggests that cross-slip of screw dislocations is severely suppressed in the MEA. In addition, among the grains with PDSs, many deformation twins were additionally observed in <1 1 1>-oriented grains, as presented in figure 4 (c).

The results described above indicate that, although the two alloys have different friction stress levels and equivalent materials properties, including SFEs, dynamic recovery (i.e., annihilation of dislocations with opposite signs through cross-slip of screw dislocations) is greatly inhibited in the MEA. One possible reason for the inhibited dynamic recovery is the effect of variation in stacking fault widths due to the local chemical environment in the MEA. Because different elements are in different lattice positions in HEAs and MEAs, SFE can be locally different, resulting in variations of stacking fault width depending on the local chemistry [15,16]. Generally, stacking faults need to shrink in the original slip plane and extend again in the cross-slip plane to allow cross-slip of screw dislocations. Therefore, it is possible that the parts of stacking faults with wider widths may be difficult to shrink, and the shrinkage of such wider parts controls the process of cross-slip of screw dislocations in HEAs and MEAs.

Another possibility is variations in stacking fault widths due to stress levels. As the SFE of the alloys used in the present study were as low as 30 $mJm^{-2}$, dislocations could dissociate into two Shockley partial dislocations. Furthermore, under uniaxial loading, the resolved shear stresses acting on the

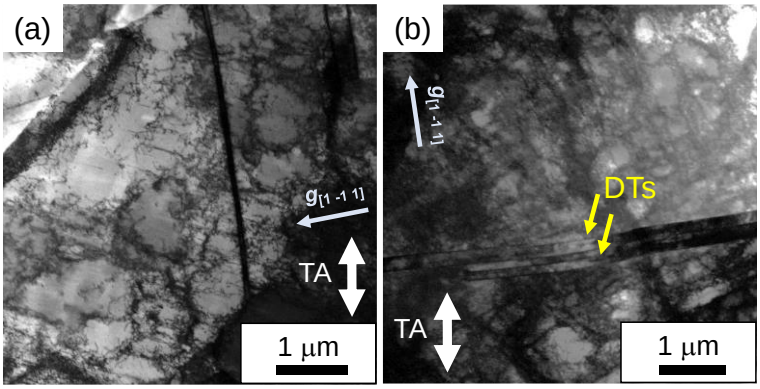


**Figure 3.** Examples of dislocation microstructures in the $Co_{60}Ni_{40}$ alloy showing (a) DCs (at a nominal strain of $e$ ~ 30%, TA ~// < 1 2 2>) and (b) DTs ($e$ ~ 50%, TA ~// <1 1 1>). TA and $g$-vector ($g_{[h\ k\ l]}$) are indicated in each image.

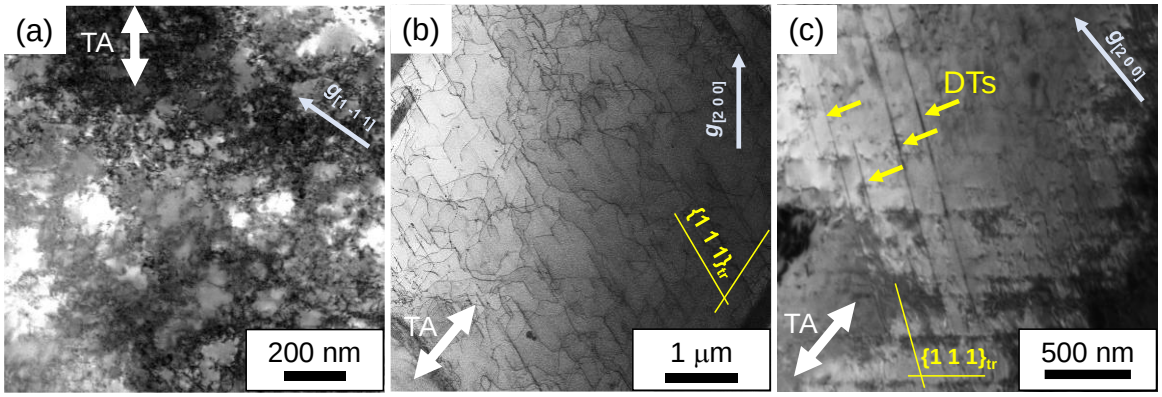


**Figure 4.** Examples of dislocation microstructures in the $Co_{20}Cr_{40}Ni_{40}$ MEA showing (a) DCs (at a nominal strain of $e$ ~ 30%, TA ~// <1 0 0>), (b) PDSs ($e$ ~ 10%, TA ~// <1 1 2>), and (c) DTs ($e$ ~ 10%, TA ~// <1 1 1>). TA and $g$-vector ($g_{[h\ k\ l]}$) are indicated in each image. The yellow lines are traces of {1 1 1} planes.

leading and trailing partial dislocations are different because they have different Burgers vectors. As a result, stacking faults can expand or shrink upon loading, and apparent SFEs (effective SFEs) can change depending on the grain orientation. Such orientation-dependent variation of effective SFEs ($\gamma_{\mathrm{eff}}$) has been formulated by Copley *et al*. [17] as follows:

$$\gamma_{\mathrm{eff}} = \gamma_0 - \frac{m_{\mathrm{L}} - m_{\mathrm{T}}}{m_{\mathrm{L}} + m_{\mathrm{T}}} \sigma b_{\mathrm{p}}, \quad (2)$$

where $\gamma_0$ is the stacking fault energy without external stress, $\sigma$ is the applied tensile stress, and $b_{\mathrm{p}}$ is the magnitude of the Burgers vector of the partial dislocations, and where $m_{\mathrm{L}}$ and $m_{\mathrm{T}}$ are the Schmid factors of the leading and trailing partial dislocations, respectively. According to equation (2), in the MEA with higher $\sigma_0$ (i.e., higher flow stress, $\sigma$), changes in effective SFEs under uniaxial stress can be more significant than in the $Co_{60}Ni_{40}$ alloy. For example, in the case of TA // <1 1 1> grains, the Schmid factor of the leading partial dislocations ($m_{\mathrm{L}}$ = 0.314) belonging to the primary slip system (the $a$/2<1 1 0>{1 1 1} slip system with the highest Schmid factor) is larger than that of the corresponding trailing partials ($m_{\mathrm{T}}$ = 0.157). Thus, stacking faults expand upon tensile loading, and the effective SFEs of the $Co_{60}Ni_{40}$ alloy and $Co_{20}Cr_{40}Ni_{40}$ MEA are calculated at their yield points as 23.1 mJm$^{-2}$ and 11.6 mJm$^{-2}$, respectively. Therefore, cross-slip of screw dislocations in the MEA is more inhibited than in the $Co_{60}Ni_{40}$ alloy, resulting in the formation of the PDSs in these grain orientations. In TA // <1 0 0>-oriented grains, the situation is the opposite: the Schmid factor of the leading partial dislocations belonging to the primary slip system ($m_{\mathrm{L}}$ = 0.236) is smaller than that of the trailing partials ($m_{\mathrm{T}}$ = 0.471), and stacking faults shrink under tensile stress. The effective SFEs of the $Co_{60}Ni_{40}$ alloy and $Co_{20}Cr_{40}Ni_{40}$ MEA are calculated at their yield point as 36.8 mJm$^{-2}$ and 48.3 mJm$^{-2}$, respectively. These SFEs might be high enough to allow cross-slip of screw dislocations forming DCs. Consequently, the orientation dependence of effective SFEs can explain the difference in the observed deformation microstructure evolution in the alloys.

As dynamic recovery was more inhibited in the $Co_{20}Cr_{40}Ni_{40}$ MEA than in the $Co_{60}Ni_{40}$ alloy, the dislocation density in the MEA can quickly increase during tensile deformation, resulting in an increase in the work-hardening rate. In addition, in grains with TA ~// <1 1 1>, dense DT boundaries introduced during deformation could have acted as further obstacles for dislocation motion and dynamically reduced the mean free path of dislocations. Although the number fraction of such grains was less than 10%, this may also have been a contributing factor to the increase in the work-hardening rate, the so-called dynamic Hall-Petch effect. Thus, we conclude that, for these reasons, the $Co_{20}Cr_{40}Ni_{40}$ MEA with high friction stress exhibited higher work-hardening ability and superior strength-ductility balance compared with the $Co_{60}Ni_{40}$ alloy. We believe that FCC high-alloy systems with high friction stress inherently develop characteristic deformation microstructures that are advantageous for realizing better mechanical properties than those in conventional FCC metals and alloys.

## 4. Conclusion

In the present study, we compared the deformation behavior of a $Co_{60}Ni_{40}$ alloy and $Co_{20}Cr_{40}Ni_{40}$ MEA with low and high friction stresses, respectively, but having otherwise similar materials properties, such as SFEs and elastic constants, and investigated the deformation microstructure evolution during tensile deformation at room temperature. The $Co_{20}Cr_{40}Ni_{40}$ MEA exhibited a higher yield strength and a higher work-hardening rate than the $Co_{60}Ni_{40}$ alloy. In the $Co_{60}Ni_{40}$ alloy, we observed coarse DCs regardless of the grain orientation, and a small number of DTs were found in a few grains oriented to TA ~// <1 1 1>. In the $Co_{20}Cr_{40}Ni_{40}$ MEA, we found fine DCs in TA ~// <1 0 0>-oriented grains, while PDSs were observed in others. Dense DTs were formed in grains oriented to TA ~// <1 1 1> in addition to the PDSs. The results indicate that cross-slip of screw dislocations (i.e., dynamic recovery during deformation) is inhibited in the MEA. This can lead to a rapid increase in dislocation density and an increase in the work-hardening rate of the MEA compared with the $Co_{60}Ni_{40}$ alloy. Therefore, characteristic deformation microstructures developed in the $Co_{20}Cr_{40}Ni_{40}$ MEA with high friction stress are beneficial for simultaneously achieving high strength and large tensile ductility.

**Acknowledgments**
This work was financially supported by the Elements Strategy Initiative for Structural Materials (ESISM, No. JPMXP0112101000), the Grant-in-Aid for Scientific Research on Innovative Area "High Entropy Alloys" (No. JP18H05455), the Grant-in-Aid for Early-Career Scientists (No. JP22K14501), the Grant-in-Aid for Research Activity Start-up (No. JP21K20487), and the Grant-in-Aid for JSPS Research Fellow (No. JP18J20766), all through the Ministry of Education, Culture, Sports, Science and Technology (MEXT), Japan. All the supports are greatly appreciated. The authors also thank Dr. Tianbo Yu and Ms. Gitte Christiansen of Technical University of Denmark (Denmark), Prof. Mitsuhiro Murayama of Virginia Polytechnic Institute and State University (USA), and Mr. Akira Yasuhara of JEOL Ltd. (Japan) for the technical supports on the transmission electron microscopy experiments.

**References**

[1] Tsai M H and Yeh J W 2014 High-Entropy Alloys: A Critical Review *Mater. Res. Lett.* **2** 107–23
[2] Miracle D B and Senkov O N 2017 A critical review of high entropy alloys and related concepts *Acta Mater.* **122** 448–511
[3] George E P, Raabe D and Ritchie R O 2019 High-entropy alloys *Nat. Rev. Mater.* **4** 515–34
[4] George E P, Curtin W A and Tasan C C 2019 High entropy alloys: A focused review of mechanical properties and deformation mechanisms *Acta Mater.* **188** 435–74
[5] Yoshida S, Bhattacharjee T, Bai Y and Tsuji N 2017 Friction stress and Hall-Petch relationship in CoCrNi equi-atomic medium entropy alloy processed by severe plastic deformation and subsequent annealing *Scr. Mater.* **134** 33–6
[6] Yoshida S, Ikeuchi T, Bhattacharjee T, Bai Y, Shibata A and Tsuji N 2019 Effect of elemental combination on friction stress and Hall-Petch relationship in face-centered cubic high / medium entropy alloys *Acta Mater.* **171** 201–15
[7] Yin B, Yoshida S, Tsuji N and Curtin W A 2020 Yield strength and misfit volumes of NiCoCr and implications for short-range-order *Nat. Commun.* **11** 2507
[8] Considère M 1885 L'emploi du fer de l'acier dans les constructions, Memoire no 34 *Ann. des Ponts Chaussées* **9** 574–775
[9] Köster E H, Thölén A R and Howie A 1964 Stacking fault energies of Ni–Co–Cr alloys *Philos. Mag.* **10** 1093–5
[10] Beeston B E P P, Dillamore I L and Smallman R E 1968 The Stacking-Fault Energy of Some Nickel-Cobalt Alloys *Met. Sci. J.* **2** 12–4
[11] Schreier H, Orteu J J and Sutton M A 2009 *Image correlation for shape, motion and deformation measurements: Basic concepts, theory and applications* (Boston: Springer US)
[12] Zhu Y, Ophus C, Toloczko M B and Edwards D J 2018 Towards bend-contour-free dislocation imaging via diffraction contrast STEM *Ultramicroscopy* **193** 12–23
[13] Huang X 1998 Grain Orientation Effect on Microstructure in Tensile Strained Copper *Scr. Mater.* **38** 1697–703
[14] Huang X and Hansen N 1997 Grain orientation dependence of microstructure in aluminium deformed in tension *Scr. Mater.* **37** 1–7
[15] Smith T M, Hooshmand M S, Esser B D, Otto F, McComb D W, George E P, Ghazisaeidi M and Mills M J 2016 Atomic-Scale Characterization and Modeling of 60° Dislocations in a High Entropy Alloy *Acta Mater.* **110** 352–63
[16] Rao S I, Woodward C, Parthasarathy T A and Senkov O 2017 Atomistic simulations of dislocation behavior in a model FCC multicomponent concentrated solid solution alloy *Acta Mater.* **134** 188–94
[17] Copley S M and Kear B H 1968 The dependence of the width of a dissociated dislocation on dislocation velocity *Acta Metall.* **16** 227–31